Supporting Information

Efficient Plasmonic Gas Sensing Based On Cavity-Coupled Metallic Nanoparticles

**Jian Qin[1], Yu-Hui Chen[2], Boyang Ding[2]*
Richard J. Blaikie[2*], and Min Qiu[1]***

[1]State Key Laboratory of Modern Optical Instrumentation, Department of Optical Engineering, Zhejiang University, Hangzhou 310027, China
[2] MacDiarmid Institute for Advanced Materials and Nanotechnology, Department of Physics, University of Otago, PO Box 56, Dunedin 9016, New Zealand

* boyang.ding@otago.ac.nz
* richard.blaikie@otago.ac.nz
* minqiu@zju.edu.cn

Section 1 Scattering Intensity of Gold Nanorods (AuNRs)

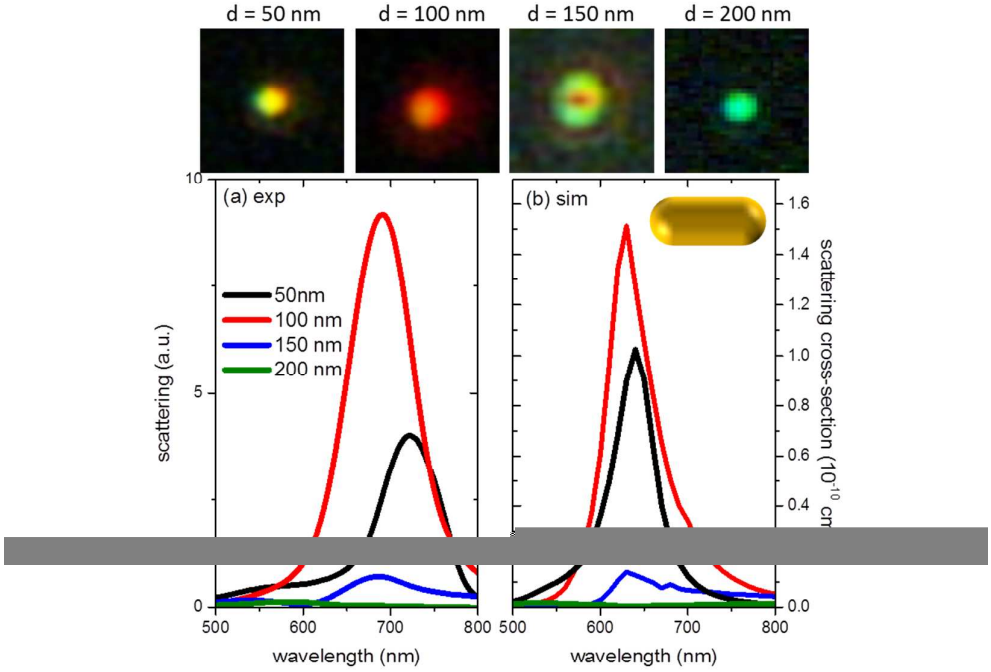

Figure S1 measured (a) and simulated (b) scattering spectra of a gold nanorod (AuNR) placed at a 50 nm (black), 100 nm (red), 150 nm (blue) and 200 nm (green) thick PVA layer on top of a gold mirror. The far-field scattering patterns of the AuNR are shown above.

Fig. S1(a) shows the measured scattering spectra of a AuNR separated from a Au mirror with varying NR-mirror distance. In our experiments, the synthesized AuNRs have a width of ~35 nm and a length of ~85 nm. We can see that the scattering spectra significantly varies with the NP-mirror distance. The simulated spectra in Fig. S1(b) exhibits very similar tendency, agreeing very well with the experimentally acquired results. The far-field patterns are also dependent on the NR-mirror distance, indicating that the NR-cavity coupling strength can be significantly modified by adjusting the NP-mirror distance.

We note that when NP-mirror distances changes from 100 nm to 150 nm, the scattering intensity greatly reduces, which is similar to the scattering variation of nanoparticles shown in the main text (Fig. 1).

Section 2 Humidity Sensing using AuNRs

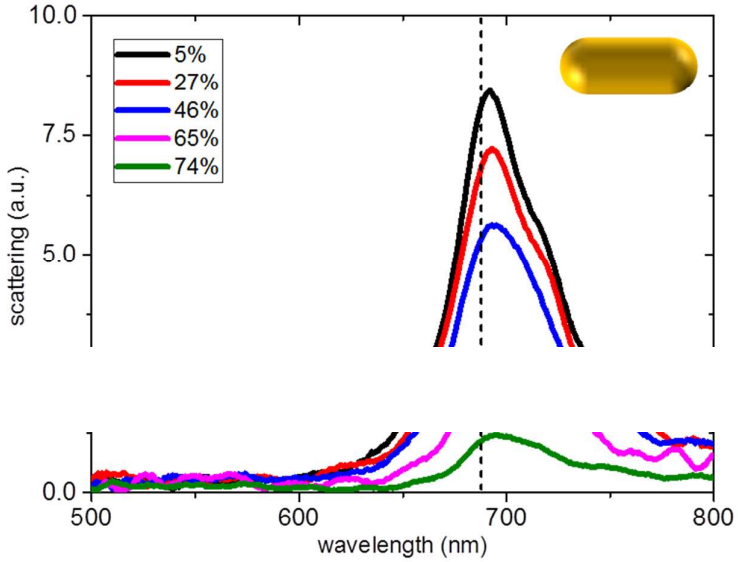

Figure S2 Measured scattering spectra of a AuNR above a Au mirror using a PVA spacer with 100 nm thickness (measured at RH = 35%) at different relative humidity (RH).

Fig. S2 shows the scattering spectra of a single AuNR placed at 100 nm above a Au mirror measured in different humidity environments. We can see that when humidity increases from 5% to 74%, the scattering magnitude of the AuNR significantly declines, exhibiting identical tendency as seen from the AuNP in the main text (Fig. 3). In particular, at the wavelength of 690 nm (as indicated by the dashed line in Fig. S2), the scattering magnitude at RH = 74% is only ~1/7.5 of the magnitude at RH = 5%, giving a sensitivity of ~12 dB/% RH. This is identical to the value achieved using a cube/sphere nanoparticles introduced in the main text, indicating that the humidity sensitivity has little relevance to the shape of nanoparticles.

The reasons behind these interesting phenomena could be manifold. First of all, the PVA expansion ability highly relates to the film's initial thickness, meaning that PVA films with different initial thickness (like in our case, 40/ 100/ 150/ 200 nm thick films) do not gain the same thickness swelling within the identical ambient humidity increment. As the result, the change of NP-mirror distance significantly differs from sample to sample. This can explain the relatively low sensitivity of samples with 40 nm PVA spacer, which has lower expansion potential.

Second, in our study, the PVA spacer thickness increases from 40 to 200 nm. This is a wide range of thickness variation, making the cavity-coupled NP structures a very complicated system for the excitation of multiple resonant optical modes. For example, when d = 40 nm, the system falls in a gap resonance regime (*J. Phys. Chem. C* 2010, 114, 7509–7514), where the electric field is highly concentrated with the spacer between NP and the mirror. For thicker spacers (d >= 100 nm), interference effects between scattered light from different interfaces starts to dominate. (*Nano Lett.* 2014, 14, 570−577) The interference effects can significantly modify the excitation of multiple optical modes in the system. For example, when the PVA thickness increases from 100 nm to 150 nm (Fig.1 in the main text), not only spectra changes, far-field scattering patterns also turn from dot-shape to doughnut shape, indicating that new optical modes with different resonant frequency and distinct polarization are excited for the d = 150 nm system. In other words, multiple optical modes can be successively excited or coexist in the studied cavity-coupled NP system as the spacer thickness changes due to various mechanisms. Arising from the interplay of the multiple modes, the linearity of scattering magnitude variations appears to be highly dependent on the spacer thickness.

Section 4 Experimental Set-up and Spectra Processing

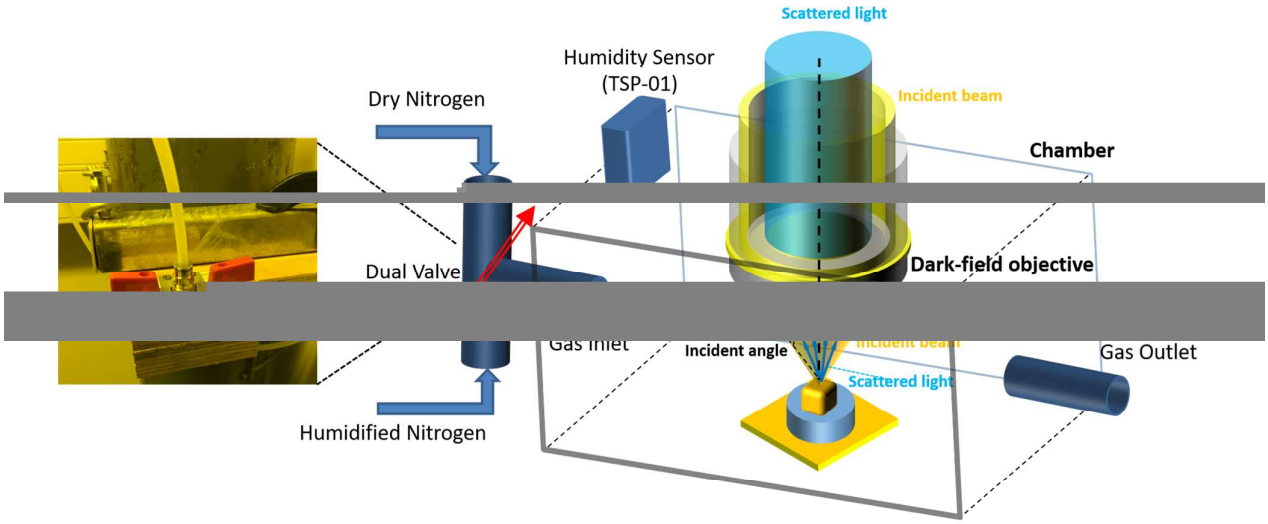

Figure S4 Schematic illustration of the experimental setup for scattering measurement of single nanoparticles and RH sensing.

Figure S4 illustrates the home-built experimental set-up for RH sensing, where a dark-field objective is sealed in a metallic chamber to collected scattered light from a single cavity-coupled NP. The scattered light is then collected and analyzed by a fiber-based spectrometer (Ocean Optics QE65 Pro, https://oceanoptics.com/wp-content/uploads/OEM-Data-Sheet-QE65Pro.pdf), while scattering image were taken by a CCD camera (Nikon, DIGITAL CAMERA HEAD DS-Fi1). The scattering spectra I_{sc} as a function of wavelength λ is acquired by using the relation $I_{sc}(\lambda) = (S - R)/R$, where S is the scattering light from an area that contains a single nanoparticle and R is the signal from a nearby area of the nanoparticle (identical sampling area but without particles).

RH inside the chamber is controlled by injecting humid nitrogen with different water vapor concentrations and is characterized by a commercial electro-chemical humidity sensor Thorlabs TSP01 (https://www.thorlabs.com/thorproduct.cfm?partnumber=TSP01). Specifically, as shown in Figure S4, dry and humidified nitrogen was mixed before being blown into the chamber through the Gas Inlet. The ratio of the mixture is controlled by a dual valve. When pure dry nitrogen is injected into the chamber, the RH value in the chamber is down to 5%; when the pure humidified nitrogen is injected, the RH value can reach up to ~80%. The chamber can be filled up very quickly (within 1 second) due to (i) the small volume of the chamber and (ii) the fast flow rate of nitrogen injection. Controlled by the dual valve, the injection of water vapor can be swiftly switched between humidified nitrogen with different RH values.

Section 5 Nanoparticles on PVA coated glass substrates

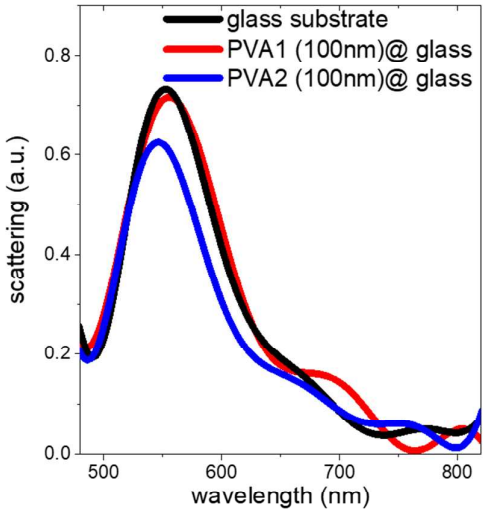

Figure S5 scattering spectrum of gold nanoparticles on a glass substrate (black), 100 nm thick PVA coated glass substrates (red and blue).

As depicted in Figure S5, the scattering spectra of AuNPs placed on 100 nm PVA coated glass substrates (red and blue curves) are almost identical to the spectrum of a AuNP directly placed on a glass substrate (black curve), indicating that the PVA-glass thin-film structure doesn't form a micro-cavity as does the PVA-Ag structure.

Section 6 PVA Thickness Dependence on Humidity

Three PVA films were coated on glass substrates. We have used an ellipsometer (Model: J.A. Woollam Co. Ellipsometry Solutions: alpha-SE) measuring their thicknesses when room RH changes. The refractive indices of PVA in different RH were acquired by interpolating data from the Ref (*Adv. Infocom Technol.* IEEE 7th International Conf. (2014) 137–142). As depicted by Table S1, the PVA thickness greatly increases as the RH value changes from ~28% to ~71%.

Section 7 Cavity-Nanoparticle Coupling

Dielectric thin-films with thickness (*d)* larger than $\lambda/4n$ (where λ is the wavelength and n is the refractive index of the film material) coated on a metallic mirror constitute an optical cavity that rely on Fabry-Perot-type interference. In particular, reflected light from the top surface (air-dielectric interface) can interact with light reflected from the bottom surface (dielectric-metal interface), leading to constructive or destructive interference depending on the coating thickness and angles and polarization of the illumination. As the result, not only the spectrum but also the electro-magnetic (EM) fields nearby the structures can be significantly modified.

In our study, a metallic nanoparticle is immobilized on the interference layers, which makes the scenario more complex. According to Ref 20 (*Nano Lett.* 2014, 14, 570−577), the physical process of the interaction between NPs and the thin-film cavity can be considered as three successive procedures: (i) light illuminating on the interference layers leads to a certain EM field distribution in the structure as described in the last paragraph; (ii) the resulting EM fields interact with the metallic NPs and induce light scattering as a result of plasmon excitation; (iii) scattered light from the NPs interferes with the bottom reflection.

This cavity-NP coupling can significantly modify the scattering pattern of NPs. For example, in our experiment (and *Nano Lett.* 2014, 14, 570−577), when $d = 150$ nm, due to interference effects in the thin-film cavity, electric fields perpendicular to the film dominates the nearby presence of the PVA surface, leading to vertical excitation of LSPs in AuNPs, thus projecting doughnut-shaped patterns in the far-field. In addition, as a result of constructive or destructive interference between scattering and bottom reflection, the scattering intensity of NPs highly depends on NP-mirror distance, which provides the basic platform for the gas-sensing application in our study.

Ref 12 (*Appl. Phys. Lett.* 2010, **97**, 253116) of the main text demonstrates another application of this cavity-NP coupling. Specifically, by using the interference layers to adjust the phase shift of plasmonic excitation, they have successfully narrowed down the linewidth of plasmonic nanorods and have used the narrowed resonance to enhance chemical sensitivity.